Numerical model evaluation of a PCM cold storage tank and uncertainty analysis of the parameters

Gabriel Zsembinszki, Pere Moreno, Cristian Solé, Albert Castell, Luisa F. Cabeza

GREA Innovació Concurrent, Universitat de Lleida, Edifici CREA, Pere de Cabrera s/n, 25001 Lleida, Spain. Tel.: +34-97-3003576; fax: +34-97-3003575. E-mail address: lcabeza@diei.udl.cat

Abstract

Thermal energy storage (TES) tanks for cold storage can be used for peak load shaving. This paper presents and evaluates a mathematical model where a TES tank is filled with commercial phase change material (PCM) flat slabs. The 2D model is used for simulating the outlet temperature of the heat transfer fluid, and also the heat transfer rate during the discharging process. The study includes the use of an approximation of the PCM specific heat ($c_{PCM;old}$) which corresponds to the parameter calculated in the previous iteration of the implicit finite difference method. Thus, an evaluation of the different model parameters is performed, based on the comparison between the computational time and accuracy of the different simulations. Moreover, the uncertainties in different input variables are also analysed in order to find out which variable should be known more accurately. The results show that using the approximated parameter $c_{PCM;old}$ is a good solution for reducing the computational time despite a slight error increase in the case of using small time step in the simulation. Moreover, the inlet HTF temperature, and melting temperature, density and specific heat of the PCM are the main parameters to take into account in terms of uncertainty variables evaluation.

Keywords: Phase change material; Thermal energy storage; Latent heat; Numerical simulations; Model optimization; HVAC systems.

1 Introduction

The use of thermal energy storage (TES) in cooling or heating systems, based on latent energy storage through phase change materials (PCM), presents some advantages such as compactness in comparison with sensible TES devices and the operational advantage of a nearly constant storage cycle-temperature [1]. A TES system based on the use of PCM can be implemented in different applications, such as solar heating installations, under floor heating, building envelopes, and HVAC systems [2-5]. Focusing only on HVAC applications, in countries where

there is a variable electricity tariff according to the consumption period, the use of a TES system offers the possibility of shifting the operating period of the system to off-peak hours, when the price of the consumed electricity is lower.

Modeling the PCM storage tanks connected to a HVAC system is important because it allows making predictions about their thermal behavior. An acceptable numerical model should be able to describe the phase change heat transfer in both melting and solidification processes with reasonable reliability, as well as to present low computing time and resources. Different models of PCM thermal storage units are available in the literature, some of them being reviewed by Lacroix [6], Verma and Singal [7] and Zalba et al. [8].

Vakilatojjar et al. [9] proposed a semi-analytical model of a slab PCM storage unit and the calculations were based on the finite elements method to predict the behaviour of the system. The unsteady two-dimensional problem was solved using the "Neumann Solution" presented by Carslaw and Jaeger [10]. Three models with different assumptions were compared in this study and they concluded that better performance of the system could be obtained by using smaller air gaps and thinner PCM slabs. Rostamizadeh et al. [11] developed a mathematical model based on an enthalpy formulation using finite difference model of an air heat exchanger when using rectangular PCM package. From the results they found a linear relationship between the mass of the PCM and the melting time.

Bony and Citherlet [12] developed a numerical model of a water tank storage implemented in an existing TRNSYS type. The model, based on the enthalpy approach, allows the simulation of the tank filled with PCM modules made of different materials and different shapes such as cylinders, plates or spheres bed. Conduction and convection inside the PCM are taken into account, as well as at the interface between PCM and water. Some experimental measurements were performed to evaluate the potential of this model, and they showed good agreement between monitored data and simulations.

Liu et al. [13] developed a one-dimensional liquid-based model which allowed for varying wall temperature along the direction of the heat transfer fluid (HTF), for analysing the thermal performance of a PCM thermal energy storage tank for cooling applications, consisting of several flat slabs parallel to each other. Two sets of experiments were used in order to validate the mathematical model, and the numerical results showed a reasonable agreement with the experimental ones in terms of outlet HTF temperature and heat transfer rate during the melting process. The model was also capable of predicting the melting time accurately. The work of Liu et al. [8] was later used in another study also by Liu et al. [14] to investigate the thermal

performance of the unit, examining the effects of the unit design and the operating parameters. In the present paper a mathematical model is presented and evaluated in terms of computational time needed by the software to simulate the system and the error produced when varying different parameters comparing with the reference case.

In most of the cases the validation of a theoretical model is done by comparison with the experimental results [12,15,16]. However, the uncertainties of the input parameters and the effect of their propagation in the simulation results are barely taken into account. An uncertainty study provides the evaluation of the uncertainty in the model outputs induced by the uncertainty in the inputs. A study of uncertainty propagation analysis was presented by Dolado et al. [17]. The authors analysed the uncertainty propagation of a theoretical model which simulated a PCM-air heat exchanger. They analysed the most significant input parameters that affect the average heat rate exchanged in the first hour of the melting stage. The results indicated that, although uncertainty of the average phase change temperature had an important effect on the uncertainty of the response, it was not advisable to invest efforts in determining this parameter with an uncertainty better than ±0.25 ºC

However, few studies in the literature have been focused on the study of uncertainty in input parameters, so further investigation is needed. In this paper, a mathematical model is developed for simulating the thermal behaviour of a TES tank for cooling applications. First, the model is evaluated in order to obtain the best relationship between computational errors and simulation time. In the second part of the paper the influence that the uncertainties in the different input variables may have on the results is evaluated, based on the comparison between the results obtained for a perturbed parameter value and the reference unperturbed case.

2 Methodology

2.1 Description and requirements of the TES unit

The system studied in this paper is a PCM thermal energy storage tank for cold storage, which could be used for cooling applications (e.g. peak load shaving of cooling device). It uses commercially available flat slab of PCM [18] in order to store latent heat through phase change of the material enclosed inside the encapsulation. The amount and properties of the PCM used in the tank, whose dimensions are 1.25×0.27×0.31 m, were determined in a previous study by Moreno et al. [19].

The system uses 12 flat slabs, parallel to each other and stacked in two columns, and the HTF is circulating through the gap that exists between the different rows of PCM slabs, as shown in Figure 1. The specifications of the PCM encapsulation are shown in Table 1.

According to the manufacturer, the PCM has a melting temperature of 10 ºC and a phase change enthalpy of 155 kJ/kg. However, experimental values of the PCM specific heat were used in the simulations, which were obtained from a DSC analysis with a Mettler-Toledo DSC 822e device and StarE v.11 software. The experimental curve showed lower melting enthalpy (around 110 kJ/kg) and a melting temperature of 11.7 ºC.

Water based HTF is employed in the system, so that the thermophysical properties of water were used in the simulations of the system for simplicity. An HTF flow rate of 0.6 m^3/hour was used in the simulation since it is a common value in heating and cooling installations.

2.2 Mathematical model

A numerical model was built for simulating the discharging process of the TES tank, i.e., process during which the PCM melts. The implicit finite differences method was used for solving the energy balance equation of each node of PCM and also of the HTF, implemented in the Engineering Equation Solver (EES) software. A two-dimensional heat transfer inside the PCM was considered here, meaning that there is a temperature gradient inside the PCM in both parallel and perpendicular directions of the HTF. On the other hand, since the gap between two different slabs is small comparing to the PCM thickness, the HTF modelling is one-dimensional. This means that there is a temperature gradient inside the HTF parallel to its flow direction. A schematic representation of the TES is shown in Figure 2.

In order to predict the thermal behaviour of the system during the discharging process different assumptions were made for simplifying the analysis:

- The thermophysical properties of the PCM are constant in the liquid and solid phases, except the specific heat c_{PCM}, which depends on the PCM temperature according to the DSC results.
- There is no heat transfer between the TES unit and the surroundings.
- All the PCM is initially at the same temperature (4.5 ºC) and in solid state. The initial temperature of the HTF inside the tank is also set to 4.5 ºC along the entire length, so that initially the PCM and HTF are in thermal equilibrium.
- All the slabs containing PCM are identical to each other, and they have symmetric thermal behaviour with respect to the horizontal plane that crosses their centre.

- Natural convection inside the PCM liquid phase is not considered.
- Thermal capacity of the encapsulation material is neglected.
- Steady state is considered during each time interval of the finite difference method.
- The simulations were run taking 8 hours as discharging time of the tank. This is because the tank could be coupled to a cooling device, so this time is considered as the working day time.

Based on these assumptions, different energy balance equations can be made for the different PCM and HTF nodes. There are 9 formally different equations for the PCM nodes, depending on the relative position of the node inside the slab, 3 different equations for the slab wall, and 3 equations for the HTF nodes. For instance, the energy balance equation for the most general inner PCM node (x,y) is presented in Equation 1, where k_{PCM} is the thermal conductivity of the PCM (W/m·K), Δx is the node length in *X* axis (m), Δy is the node height in *Y* axis (m), ρ_{PCM} is the PCM density (kg/m^3), c_{PCM} (*x*,y) is the specific heat of the PCM node (x,y) (J/kg·K), T_{PCM} (*x*,y) is the temperature of the PCM node (*x*,y), and $T_{PCM;old}$ (x,y) is the PCM temperature of the node (x,y) in the previous iteration:

$$k_{PCM}\cdot\Delta y\cdot\left[\frac{T_{PCM}(x-1,y)-T_{PCM}(x,y)}{\Delta x}\right]+k_{PCM}\cdot\Delta y\cdot\left[\frac{T_{PCM}(x+1,y)-T_{PCM}(x,y)}{\Delta x}\right]+k_{PCM}\cdot\Delta x\cdot$$
$$\cdot\left[\frac{T_{PCM}(x,j-1)-T_{PCM}(x,y)}{\Delta y}\right]+k_{PCM}\cdot\Delta x\cdot\left[\frac{T_{PCM}(x,y+1)-T_{PCM}(x,y)}{\Delta y}\right]=\rho_{PCM}\cdot\Delta x\cdot\Delta y\cdot c_{PCM}(x,y)\cdot$$
$$\left[\frac{T_{PCM}(x,y)-T_{PCM,old}(x,y)}{\Delta t}\right] \quad \text{Equation (1)}$$

In a similar way, the energy balance equation for a general wall node *x* is given in Equation 2, where h_{HTF} is the convection heat transfer coefficient between the HTF and the wall (W/m^2·K), T_{HTF} (x) is the HTF temperature of node *x*, T_s (*x*) is the wall temperature of the x position, k_{wall} is the thermal conductivity of the wall (W/m·K), T_{PCM} (x,1) is the temperature of the PCM node (x,1) that is in direct contact with the wall, and d_{wall} is the wall thickness (m):

$$h_{HTF}\cdot\Delta x\cdot(T_{HTF}(x)-T_s(x))+k_{wall}\cdot\Delta x\cdot\left[\frac{T_{PCM}(x,1)-T_s(x)}{d_{wall}}\right]+k_{wall}\cdot d_{wall}\cdot\left[\frac{T_s(x+1)-T_s(x)}{\Delta x}\right]+$$
$$k_{wall}\cdot d_{wall}\cdot\left[\frac{T_s(x-1))-T_s(x)}{\Delta x}\right]=0 \quad \text{Equation (2)}$$

Finally, the energy balance equation for a general node of HTF is shown in Equation 3, where ΔA is the contact surface area between slabs walls and HTF (m^2), corresponding to position x, $\dot{m}$ is the mass flow rate of HTF (kg/s), ρ_{PCM} is the HTF density (kg/m^3), c_{HTF} is the specific heat of the HTF (J/kg·K), H is the height of the duct where the HTF flows, which is equal to the

separation between the slabs rows (m), Δt is the time step of the numerical method (s), and $T_{HTF;old}(x)$ is the HTF temperature in the x position of the previous iteration:

$$h_{HTF} \cdot \Delta A \cdot (T_s(x) - T_{HTF}(x)) + \dot{m} \cdot c_{HTF} \cdot (T_{HTF}(x-1)) - T_{HTF}(x)) = \rho_{HTF} \cdot \Delta A \cdot c_{HTF} \cdot \frac{H}{2} \cdot \left[\frac{T_{HTF}(x) - T_{HTF,old}(x)}{\Delta t}\right] \quad \text{Equation (3)}$$

The convection heat transfer coefficient h_{HTF} between slab wall and HTF is calculated by means of a procedure available in the EES software, which requires as input data the Reynolds and Prandtl numbers evaluated at the HTF bulk temperature, the ratio of tube length to hydraulic diameter, the ratio of the minimum to maximum dimension of duct, and the relative roughness of the tube wall. The procedure returns two Nusselt numbers for a given flow condition in a rectangular duct. One corresponds to a constant temperature wall and gives the lowest limit of this parameter, while the other corresponds to a constant heat flux and gives the highest value. In this study the constant temperature wall condition was assumed since this condition is more suitable when a phase change process occurs, but one should keep in mind that the actual Nusselt number may take any value between these two extreme limits.

The instantaneous heat transfer rate during the discharging (PCM melting) process is inferred by means of Equation (4), which supposes that the heat transfer rate transferred by the HTF is equivalent to a temperature decrease between inlet and outlet:

$$\dot{Q} = \dot{m} \cdot c_{HTF} \cdot \left(T_{HTF;in} - T_{HTF;out}\right) \quad \text{Equation (4)}$$

2.3 Numerical model evaluation

The numerical model has different parameters that may affect results accuracy and also the time required by the simulations. It is expected that a high accuracy implies a large computing time and, equivalently, a short computing time leads to less precise and reliable results. For this reason, a first step was to find the best combination of parameter values, able to make acceptably accurate predictions with a reasonable computing time.

There are mainly three parameters that affect the precision and time of the simulations: the number of PCM nodes N_x and N_y along the horizontal *X*-axis and vertical *Y*-axis, respectively, and the time step Δt of the iteration process. Since the implicit finite difference method is used here, the time step is in principle unconditionally steady, and there is no limit for its value. This

is why the minimum value for Δt = 4 s considered here corresponds to the limitations of the software computing capacity.

Another issue related to the numerical model that was investigated was the use of some simplifications, aiming to reduce the computing time without affecting too much the precision. One of such simplifications consisted in the use of the PCM specific heat $c_{PCM;old}$. This parameter corresponds to the specific heat calculated in the previous iteration of the implicit finite difference method, instead of using c_{PCM} which is evaluated at the present iteration as a function of the (unknown yet) PCM node temperature. The temperatures are updated in the present iteration when this simplification is used.

In order to find the better setup of model parameter values, three different values were considered for each parameter, and the model was then tested for all the possible combinations. For the number of PCM nodes N_x and N_y the values of 16, 10 and 4 were considered, while for the time step Δt the values 4, 30 and 300 s were taken. As previously mentioned, Δt = 4 s corresponds to the limitations of the software computing capacity, 30 seconds can be a suitable value for experimental data logging, and 300 seconds was selected as maximum time step. Each combination of parameter values was tested both for the specific heat c_{PCM}, and for the approximation $c_{PCM;old}$. With all this, a total of 54 different combinations were obtained and tested, using an ordinary Sony VAIO laptop with an Intel(R) Core(TM)2 Duo CPU T5800 @ 2.00 GHz processor and 3.00 GB of RAM.

The combination of parameter values, which should give the most precise results and also the largest computing time, is the one that has the highest number of PCM nodes and the least time step, i.e., $N_x = N_y = 16$, Δt = 4 s, and the use of c_{PCM} as the specific heat of the PCM. This combination was taken as the reference case and, although the results provided by this configuration are not free of error, it was supposed small and it was neglected. The results of the simulations inferred by the other cases were compared to the reference case. In order to quantify the precision of the different cases, specific statistical variables may be used. In this case, one is interested in comparing the predictions of different cases with the results of the reference case, so that mean absolute deviation (MAD) and mean absolute percentage error (MAPE) were chosen as measures of prediction accuracy. The first parameter gives an idea of the error in $T_{HTF;out}$, and has the advantage that it is an absolute error (and expressed in ºC) that can be compared to the precision of ordinary temperature probes used in real installations. If MAD is lower than this precision, then the case evaluated has acceptable error.

The MAD of the outlet HTF temperature $T_{HTF;out}$ can be calculated by means of Equation (5), where the superscript "sim" refers to the value predicted by the simulation, the superscript "ref" means the value of the reference case, and n = (8 hours)/Δt is the number of iteration points:

$$MAD = \frac{1}{n}\sum_{i=1}^{n}\left(T_{HTF;out}^{sim,i} - T_{HTF;out}^{ref,i}\right) \quad \text{Equation (5)}$$

The MAPE measure is useful when the absolute value of the variable error is not of interest, but the relative error. In our case the interest lies in the evaluation of the MAPE by using the heat transfer rate since it is the main output parameter to evaluate the discharging process. Thus, the MAPE defined in Equation (6) was used for estimating the accuracy of the simulated heat transfer rate Q^{sim}:

$$\mathrm{MAPE} = \frac{1}{n}\sum_{i=1}^{n}\left(\frac{Q^{sim,i} - Q^{ref,i}}{Q^{ref,i}}\right)\cdot 100\ \% \quad \text{Equation (6)}$$

Finally, in order to find out the most appropriate values of the model parameters to be used for further analysis, both computing time and accuracy must be taken into account. Therefore, the product between the computing time and the MAPE was also calculated, as shown in Equation (7):

$$\mathrm{Product} = \frac{\mathrm{Time}\cdot\mathrm{MAPE}}{100\ \%} \quad \text{Equation (7)}$$

The cases that minimize this parameter should be the ones to be taken into consideration for deciding the final configuration of model parameters.

2.4 Analysis of uncertainties in input variables

After evaluating the numerical model, the second step consisted of studying the effect that uncertainties in some of the input variable might have on the estimated results. There are different parameters that introduce uncertainty in the results, which were considered and classified into three groups:

(i) PCM properties: density, specific heat, thermal conductivity, and melting temperature;

(ii) HTF properties: density, specific heat, flow rate and inlet temperature;

(iii) Heat transfer: convection coefficient between HTF and wall surface, and slab wall thermal conductivity.

The main source of uncertainties in these variables consists in the experimental measurement of material properties. When measuring the density and the specific heat of a PCM, the typical uncertainty ranges between 3–5% [20,21], so the larger value of 5% was considered in this study. The melting temperature of PCM may also be affected by experimental errors, and ±1ºC was supposed as uncertainty of T_{melt}.

In the case of the HTF properties, its density and specific heat depend on the bulk temperature of the HTF, which is inferred by means of Equation (8), where $T_{HTF;in}$ is the inlet temperature of the current iteration, and $T_{HTF;out;old}$ is the outlet temperature of the HTF, calculated in the previous iteration.

$$T_{bulk} = \frac{T_{HTF;in} + T_{HTF;out,old}}{2} \quad \text{Equation (8)}$$

In this paper the properties of the HTF were considered the same as for water evaluated at HTF bulk temperature, but one should take into account that they can be different, because the HTF may contain some additives in low concentrations. Since *a priori* these uncertainties are unknown, an error of ±5 % of the parameter value was considered, which is the same as for the PCM properties.

An error in the HTF flow rate can also be considered for the simulations. In this study the chosen value was ±5%, which is slightly higher than accuracy of commercial flow meters (usually around ±2%).

Regarding the inlet HTF temperature, a function approximation to linear dependence with time, from about 5 ºC initially to around 25 ºC after the period of 8 hours, was considered. The function is shown in Equation (9), where *t* is expressed in hours and varies between 0 and 8:

$$T_{HTF;in}(t) = 5 + 2.5 \cdot t \quad \text{Equation (9)}$$

Nevertheless, this temperature evolution is a rough assumption and a real implementation of the system would probably have a distinct temperature profile. For this reason, an uncertainty of 1 ºC in $T_{HTF;in}$ was considered here.

The convection heat transfer coefficient h_{HTF} is estimated by means of procedures defined in EES software, which are based on empirical correlations and may also be affected by errors. Moreover, the geometrical characteristics of the ducts where the HTF flows may be slightly

different than supposed here, and the uncertainties in the HTF properties may also affect the estimated value for h_{HTF}. As mentioned in Section 2.2 the value of the Nusselt number can vary between two extreme values given by the assumption of constant surface temperature and constant heat flux. The authors checked that the difference between them may be of the order of 60 %. Consequently, an uncertainty of ±30% of the value given by the EES software was assumed for h_{HTF}.

Finally, the thermal conductivity of the slab wall is another parameter that introduces uncertainties in the model. The heat transfer through the slab wall is affected by different factors such as uncertainties in the wall thickness, or the existence of a contact resistance inside the slab, between the wall and the PCM. Thus, an uncertainty of ±5% was considered for the effective thermal conductivity of the slab wall.

The reference values considered for the main inlet variables, along with their uncertainties, are summarized in Table 2.

In order to study the effect of uncertainties in the inlet variables, different cases were prepared by making all the possible combinations of parameter values. The reference case corresponds to the reference values of the parameters shown in Table 2. The other cases were obtained from the reference one, by only modifying one parameter, while the rest of parameter values were left unchanged. Two cases were generated for each parameter, corresponding to the two extreme values of the uncertainty interval. Once all the cases were prepared, the model was first run for the reference configuration, followed by the other 20 cases, and the results of the simulations were then compared to the reference case.

As a measure of precision of each simulation, the MAPE in the heat transfer rate was calculated, as shown in Equation (6). Another magnitude of interest was considered, the percentage error (PE) of the average heat transfer rate, defined in Equation (10), which is useful for measuring the accuracy of the predictions for the total heat exchanged in the entire discharging process.

$$\mathrm{PE} = \frac{Q^{sim}_{average} - Q^{ref}_{average}}{Q^{ref}_{average}} \cdot 100\ \% = \frac{\sum_{i=1}^{n}(Q^{sim,i} - Q^{ref,i})}{\sum_{i=1}^{n} Q^{ref,i}} \cdot 100\ \% \qquad \text{Equation (10)}$$

3 Results and discussion

3.1 Selection of parameter values

Different simulations were performed for all 54 cases obtained by combining all the possible values of the model parameters. For each simulation the computing time was registered, and the MAPE of the heat transfer rate was calculated in terms of the best case, which was taken as the reference case. The results of the simulations are shown in Table 3.

The MAD of the outlet HTF temperature $T_{\mathrm{HTF;out}}$ was also calculated, and one obtained that it was less than 0.05 ºC for all the simulations, which is an acceptable error.
From Table 3 it can be observed that the reference case required the largest computational time, with more than 1 hour, which is by far too high as to be considered suitable, despite the fact that it is the most precise. One also can observe that the use of the $c_{PCM;old}$ approximation leads to a significant reduction of the computing time in all cases, while the error generally increases except for a few cases where it actually decreases. Notice that the MAPE does not exceed 2.5% in any case , meaning that even with a poor choice of parameter values the predictions of the numerical model are quite good.

Next, it was necessary to decide which of the above results was the most appropriate to be used for further investigations. Since the ideal model should have the smallest error with the lowest computing time, the selection criterion for searching the best case was that the product of computing time and error was minimum. Table 4 presents the results of the product (Time × MAPE)/100% for all cases.

The results shown in Table 4 indicate that the best combinations correspond to the largest time step Δt = 300 s and N_{x} = 4 or N_{x} = 10 with N_{y} = 4, especially due to a very short computing time while the errors are not too large. On the other hand, still good choices could be the combination with Δt = 4 s, N_{x} = 16, N_{y} = 16 or 10 and the use of the $c_{PCM;old}$ approximation, but their computing time is unacceptably long.

However, taking 300 seconds as time step is not a suitable option when experimental studies are carried out, so in that regard Δt = 30 s was considered to be more valid for further work. With this selection there are 5 cases having the minimum value of 0.6, so that any of these combinations could be a good choice. The two cases with N_{x} = 16 require the longest computing time, more than 5 minutes, and were rejected. The remaining three options are very similar; one

of them has longer computing time but smaller error, the second one has shorter computing time and higher error, while the last one has intermediate time and error. Since there is no preference between time and error, the combination with N_x = 10, N_y = 10 and $c_{PCM;old}$ was finally chosen as the better combination of parameter values, and was considered for subsequent investigations.

3.2 Uncertainties in input variables

After having evaluated the parameters of the numerical model, it was used for testing the influence of uncertainties in the different inlet variables on the results. The model was first run to obtain the reference curves of the outlet HTF temperature and the instantaneous heat transfer rate. The results are presented in Figure 3.

The average heat transfer rate during the 8 hours considered for the discharging process for the reference case was $Q_{average}$=354.8 W, equivalent to a total heat transfer of 1.02×10^7 J or 2.84 kWh. Afterwards, the model was run for the other cases, and the simulated results were compared to the reference case. The MAPE of the instantaneous heat transfer rate, and also the PE of the average heat transfer rate over 8 hours were then calculated in order to check the deviations with respect to the reference case. The results obtained for all the runs are shown in Table 5.

Table 5 shows that the maximum MAPE with respect to the reference case corresponds to the inlet HTF temperature $T_{HTF;in}$, which means that it is important to know the profile of this variable in order to obtain an accurate prediction for the heat transfer rate over the discharging period. This profile can be obtained by direct measurement of $T_{HTF;in}$, and if the "exact" measured values are within the ±1ºC uncertainty interval of the linear dependence shown in Equation (8), one should expect deviations less than the values shown in Table 5 for MAPE and PE. It should be remarked that although the MAPE in this case is relatively large, the PE of the average heat transfer rate is lower, and it is comprised within the interval ±3.4% with respect to the reference case. This means that the profile of the heat transfer rate is quite different with respect to the reference, though the total heat interchanged in the process is not too different (see Figure 4).

Another inlet variable that may affect the heat transfer profile is the PCM melting temperature, with a MAPE around 5%. Figure 5 shows the heat transfer rate for the cases in which the PCM melting temperature is 1ºC below or above the reference case, and also the reference curve.

Again, in this case the PE of the average heat transfer rate is lower than the MAPE, and the error in the prediction of the total heat interchanged is less than 2%.

The uncertainty in the PCM density and specific heat are also important, and from Table 5 one can see that they affect the results by 3.4%, both in MAPE and PE. This means that in this case although the profile of the heat transfer rate remains similar to the reference, it is shifted upwards or downwards due the uncertainties in ρ_{PCM} and c_{PCM}.

Uncertainties in the density and specific heat of the HTF are less important, producing a MAPE and PE of about 1.5%, which suggested that, in order to reduce the computing time, they could be considered constant for all the discharging process. In order to check that statement, another test was done with the simplifying assumption that T_{bulk} = 15 ºC, and all HTF properties were evaluated at this temperature. With this simplification, the computing time reduced to less than a half (Time = 98.7 s vs. 213 s), while the errors of the simulated heat transfer rate only increased slightly (MAPE = 0.327% vs. 0.303%), so that the product of time and error reduced at half: (Time × MAPE)/100% = 0.3 vs. 0.6. This result indicates that assuming constant HTF properties evaluated at the average temperature of the process (= 15 ºC) is a good option for considerably reducing the time, at the expense of a slight increase of the errors.

The uncertainties in the other input variables, i.e. PCM thermal conductivity k_{PCM}, HTF flow rate V, convection heat transfer coefficient h_{HTF}, and slab wall thermal conductivity k_{wall}, have a tiny effect on the results, especially on the PE of the average heat transfer rate, which is practically equal to that of the reference case.

4 Conclusions

A two-dimensional numerical model was developed and analysed in this paper for predicting the thermal behaviour of a cold storage tank, based on the use of PCM encapsulated in parallel flat slabs. Implicit finite difference method was used for predicting the outlet HTF temperature, and also the heat transfer rate during the discharging process. The computational time and the accuracy of the predictions were analysed for different cases obtained as combinations of parameter values, in order to find the best configuration of the model.

It was found that using a small time step and a large number of PCM nodes one gets more accurate predictions, but the computing time is too long. However, the results showed that it is not worth using small time steps and a large number of nodes, since reasonable accurate predictions can still be obtained by using a time step as large as 300 s, and only 4 nodes in each

direction, while the computing time reduces drastically by 99.68% with respect to the reference case.

The use of some simplifying approximations was also investigated, such as the use of $c_{PCM;old}$, or constant HTF properties. Using $c_{PCM;old}$ is a good solution for reducing the computational time despite a slight error increase in the case of using small time step in the simulation (e.g. Δt=4 s). If one is more interested in having a short computing time rather than accurate results, further approximations such as the use of constant HTF properties can be used.

The influence of uncertainties in some of the input variables were also studied, in order to quantify their effect on the predictions, and also to find out which input variables should be known more accurately. Attention should be paid to the inlet HTF temperature profile, and also to some of the PCM properties, such as melting temperature, density, and specific heat.

Acknowledgements

The research leading to these results has received funding from the [European Community's] Seventh Framework Programme ([FP7/2007-2013] [FP7/2007-2011]) under grant agreement nº262285. The work was partially funded by the Spanish government (ENE2011-22722, ENE2011-28269-C03-01 and ULLE10-4E-1305). The authors would like to thank the Catalan Government for the quality accreditation given to their research group (2009 SFR 534).

References

[1] I. Dincer and M.A. Rosen, Thermal enery storage: Systems and Applications, first ed., John Wiley & Sons, Baffins Lane, England, 2002.

[2] F. Niu, L. Ni, Y. Yaio, Y. Yu, H. Li, Performance and thermal charging/discharging features of a phase change assisted heat pump system in heating mode, Appl. Therm. Eng. 58 (2013) 536-541.

[3] K. Nagano, S. Takeda, T. Mochida, K. Shimakura, T. Nakamura, Supply of a floor air conditioning system using granular phase change material to augment building mass thermal storage – Heat response in small scale experiments, Energ. Buildings 38 (2006) 436-446.

[4] C. Castellón, A. Castell, M. Medrano, I. Martorell, L.F. Cabeza, Experimental study of PCM inclusion in different buildings envelopes, J. Sol. Energ.-T. ASME 131 (2009) 0410061-0410066.

[5] G. Fang, S. Wu, X. Liu, Experimental study on cool air-conditioning system with spherical capsules packed bed, Energ. Buildings 42 (2010) 1056-1062.

[6] M. Lacroix, Modeling of latent heat storage systems, in: John Wiley & Sons, Thermal Energy Storage, Systems and Applications, Baffins Lane, England, 2002, pp. 303-335.

[7] P. Verma, Varun, S.K. Singal, Review of mathematical modeling on latent heat thermal energy storage systems using phase-change material, Renew. Sust. Energ. Rev. 12 (2008) 999–1031.

[8] B. Zalba, J.M. Marín, L.F. Cabeza, H. Mehling, Review on thermal energy storage with phase change: materials, heat transfer analysis and applications, Appl. Therm. Eng. 23 (2003) 251–283.

[9] S.M. Vakilaltojjar, W. Saman, Analysis and modelling of a phase change storage system for air conditioning applications, Appl. Therm. Eng. 21 (2001) 249-263.

[10] H.S. Carslaw, J.C. Jaeger, Conduction of Heat in Solids, second ed., Clarendon Press, Oxford, 1959.

[11] M. Rostamizadeh, M. Khanlarkhani, S. MojtabaSadrameli, Simulation of energy storage system with phase change material (PCM), Energ. Buildings 49 (2012) 419-422.

[12] J. Bony, S. Citherlet, Numerical model and experimental validation of heat storage with phase change materials, Energ. Buildings 39 (2007) 1065–1072.

[13] M. Liu, W. Saman, F. Bruno, Validation of a mathematical model for encapsulated phase change material flat slabs for cooling applications, Appl. Therm. Eng. 31 (2011) 2340-2347.

[14] M. Liu, F. Bruno, W. Saman, Thermal performance analysis of a flat slab phase change thermal storage unit with liquid-based heat transfer fluid for cooling applications, Sol. Energy 85 (2011) 3017-3027.

[15] P. Dolado, A. Lazaro, J.M. Marin, B. Zalba, Characterization of melting and solidification in a real scale PCM-air heat exchanger: Numerical model and experimental validation, Energ. Convers. Manage. 52 (2011) 1890-1907.

[16] A. El-Sawi, F. Haghighat, H. Akbari, Centralized latent heat thermal energy storage system: Model development and validation, Energ. Buildings 65 (2013) 260-271.

[17] P. Dolado, J. Mazo, A. Lázaro, J.M. Marín, B. Zalba, Experimental validation of a theoretical model: Uncertainty propagation analysis to a PCM-air thermal energy storage unit, Energ. Buildings 45 (2012) 124-131.

[18] PCM Products, www.pcmproducts.net.

[19] P. Moreno, C. Solé, A. Castell, L.F. Cabeza, Design of PCM Thermal Storage Units for a HVAC system, Proceedings of Innostock 2012-12th International Conference on Energy Storage, Lleida, Spain.

[20] G.W.H. Höhne, W. Hemminger, H.J. Flammerscheim, in: Differential Scanning Calorimetry, Springer, Berlin (Germany), 1996, Chapter 6.

[21] S. Rudtsch, Uncertainty of heat capacity measurements with differential scanning calorimeters, Thermochim. Acta 382 (2002) 17-25.

Nomenclature

ΔA	Contact surface area m^2
Δt	Time step s
Δx	Node length in X axis m
Δy	Node length in Y axis m
c	Specific heat J kg^{-1} K^{-1}
d	Wall thickness m
h	Convection heat transfer coefficient W m^{-2} K^{-2}
H	Height of the duct m
(x,y)	Node (x,y)
k	Thermal conductivity W m^{-1} K^{-1}
$\dot{m}$	Mass flow rate kg s^{-1}
N_x	Nodes in vertical X-axis
N_y	Nodes in horizontal Y-axis
Q	Heat transfer rate W
ρ	Density kg· m^{-3}
t	time h
T	Temperature ºC
$\dot{V}$	Volumetric flow rate m^3 h

Subscript

average	Average
bulk	Bulk
HTF	Heat transfer fluid
in	Inlet
old	Previous iteration
out	Outlet
melt	Melting
PCM	Phase change material
s	Surface of the encapsulation wall
wall	Encapsulation wall

Superscript

sim,i	Predicted value by the simulation
ref,i	Reference case

Abbreviations

MAD	Mean absolute deviation
MAPE	Mean absolute percentage error
PE	Percentage of error

Figure captions

Figure 1. Schematics of the PCM flat slabs distribution in the TES tank (left) and image of two PCM flat slabs (right).

Figure 2. Schematic representation of the TES.

Figure 3. Reference curves for the outlet HTF temperature and for the heat transfer rate.

Figure 4. Heat transfer rate for different inlet HTF temperature.

Figure 5. Heat transfer rate for different PCM melting temperatures.

Table 1. Flat PCM encapsulation specifications

Parameter	Value
Flat length (m)	0.5
Flat width (m)	0.25
Flat thickness (m)	0.032
Gap (m)	0.013

Table 2. Reference parameter values and uncertainties

Variable	ρ_{PCM}	k_{PCM}	c_{PCM}	T_{melt}	ρ_{HTF}	c_{HTF}	$\dot{V}$	$T_{HTF;in}$	h_{HTF}	k_{wall}
Units	kg/m^3	W/m·K	J/kg·K	ºC	kg/m^3	J/kg·K	m^3/h	ºC	W/m^2·K	W/m·K
Reference value	1470	0.43	DSC curve	11.7	Water at T_{HTF}	Water at T_{HTF}	0.6	Eq.(9)	Given by EES	0.5
Error	±5%	±5%	±5%	±1	±5%	±5%	±5%	±1	±30%	±5%

Table 3. Computing time and MAPE of the heat transfer rate with respect to the reference case

			N_x=16		N_x=10		N_x=4	
			c_{PCM}	$c_{PCM;old}$	c_{PCM}	$c_{PCM;old}$	c_{PCM}	$c_{PCM;old}$
Δt=4 s	N_y=16	Time (s)	3890	2572	2643	1835	1603	1406
		MAPE (%)	*Reference*	0.015	0.128	0.144	0.671	0.686
	N_y=10	Time (s)	3097	1838	1961	1531	1147	1000
		MAPE (%)	0.029	0.026	0.11	0.124	0.649	0.664
	N_y=4	Time (s)	1624	1319	1321	1147	923	864
		MAPE (%)	0.403	0.388	0.307	0.302	0.453	0.465
Δt=30 s	N_y=16	Time (s)	617	339	395	258	244	205
		MAPE (%)	0.125	0.203	0.210	0.320	0.717	0.830
	N_y=10	Time (s)	433	319	284	213	191	158
		MAPE (%)	0.129	0.190	0.199	0.303	0.699	0.812
	N_y=4	Time (s)	225	183	181	161	126	118
		MAPE (%)	0.473	0.409	0.385	0.374	0.531	0.626
Δt=300 s	N_y=16	Time (s)	68.6	39.9	49.5	27.2	28.9	17.7
		MAPE (%)	1.03	1.775	1.056	1.872	1.278	2.304
	N_y=10	Time (s)	51.6	32.3	31.8	22.4	20.2	15.8
		MAPE (%)	1.033	1.762	1.058	1.859	1.274	2.287
	N_y=4	Time (s)	22.6	17.3	18.3	14.7	13.6	12.3
		MAPE (%)	1.114	1.616	1.099	1.705	1.241	2.105

Table 4. Results for (Time × MAPE)/100%

		N_x=16		N_x=10		N_x=4	
		c_{PCM}	$c_{PCM;old}$	c_{PCM}	$c_{PCM;old}$	c_{PCM}	$c_{PCM;old}$
Δt=4 s	N_y=16	*Reference*	0.4	3.4	2.6	10.8	9.6
	N_y=10	0.9	0.5	2.2	1.9	7.4	6.6
	N_y=4	6.5	5.1	4.1	3.5	4.2	4.0
Δt=30 s	N_y=16	0.8	0.7	0.8	0.8	1.7	1.7
	N_y=10	0.6	0.6	0.6	0.6	1.3	1.3
	N_y=4	1.1	0.7	0.7	0.6	0.7	0.7
Δt=300 s	N_y=16	0.7	0.7	0.5	0.5	0.4	0.4
	N_y=10	0.5	0.6	0.3	0.4	0.3	0.4
	N_y=4	0.3	0.3	0.2	0.3	0.2	0.3

Table 5. Average heat transfer rate and deviations produced by uncertainties

Variable	Units	Reference value	Tested value	$Q_{average}$ (W)	MAPE (%)	PE (%)
ρ_{PCM}	kg/m^3	1470	1543.5	367.0	3.4	3.4
			1396.5	342.5	3.4	–3.4
k_{PCM}	W/m·K	0.43	0.45	355.0	0.6	0.1
			0.41	354.5	0.7	–0.1
c_{PCM}	J/kg·K	DSC curve	Ref. + 5%	367.0	3.4	3.4
			Ref. – 5%	342.5	3.4	–3.4
T_{melt}	ºC	11.7	12.7	360.1	5.1	1.5
			10.7	348.3	4.7	–1.8
ρ_{HTF}	kg/m^3	Water at T_{HTF}	Ref. + 5%	359.9	1.5	1.4
			Ref. – 5%	349.6	1.5	–1.5
c_{HTF}	J/kg·K	Water at T_{HTF}	Ref. + 5%	359.9	1.5	1.4
			Ref. – 5%	349.6	1.5	–1.5
$\dot{V}$	m^3/h	0.6	0.63	354.9	0.3	0.0
			0.57	354.6	0.3	–0.1
$T_{HTF;in}$	ºC	Eq. (9)	Ref. + 1	366.7	11.0	3.4
			Ref. – 1	342.6	11.2	–3.4
h_{HTF}	W/ m^2·K	Given by EES	Ref. + 30%	355.2	1.5	0.1
			Ref. – 30%	353.9	2.6	-0.3
k_{wall}	W/m·K	0.5	0.525	354.8	0.2	0.0
			0.475	354.7	0.2	0.0

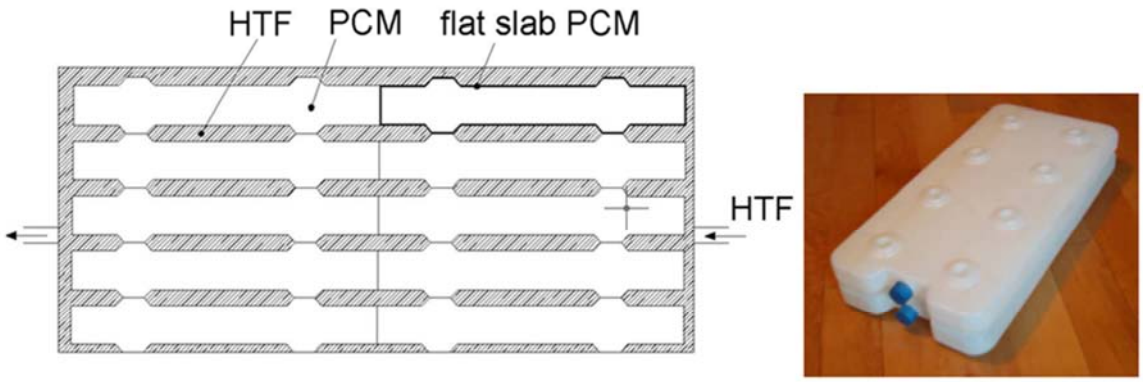

Figure 1

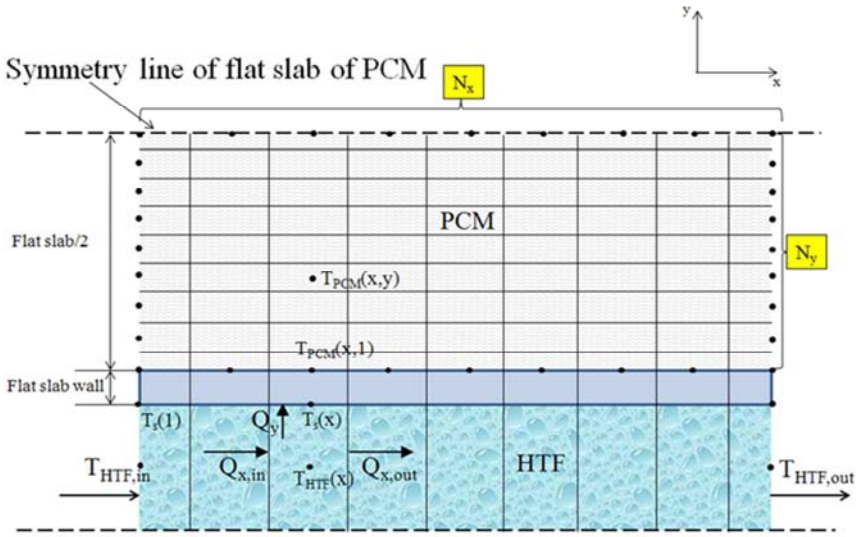

Figure 2

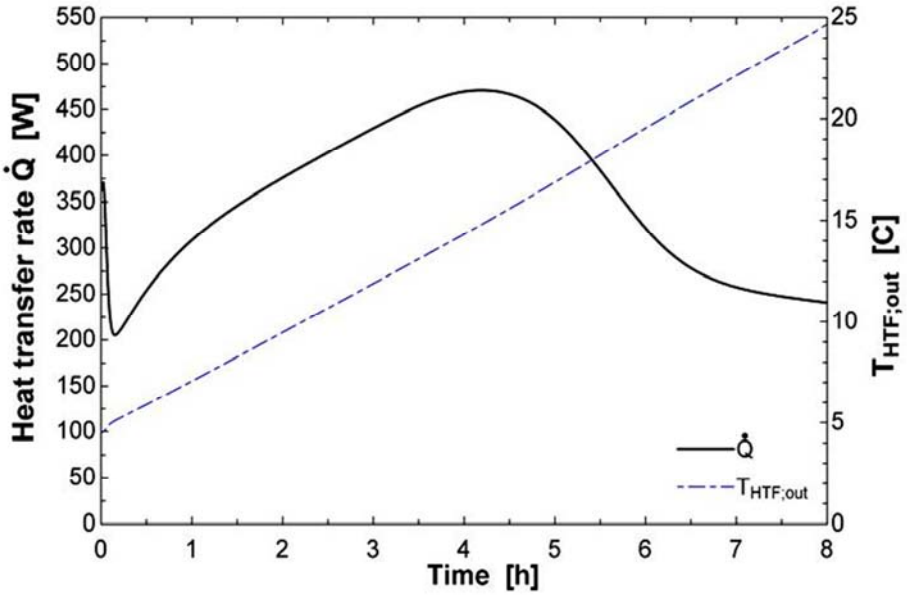

Figure 3

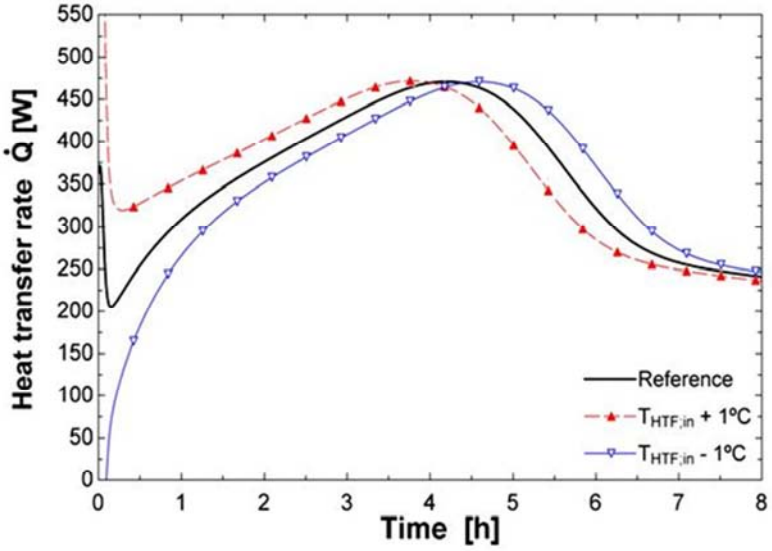

Figure 4

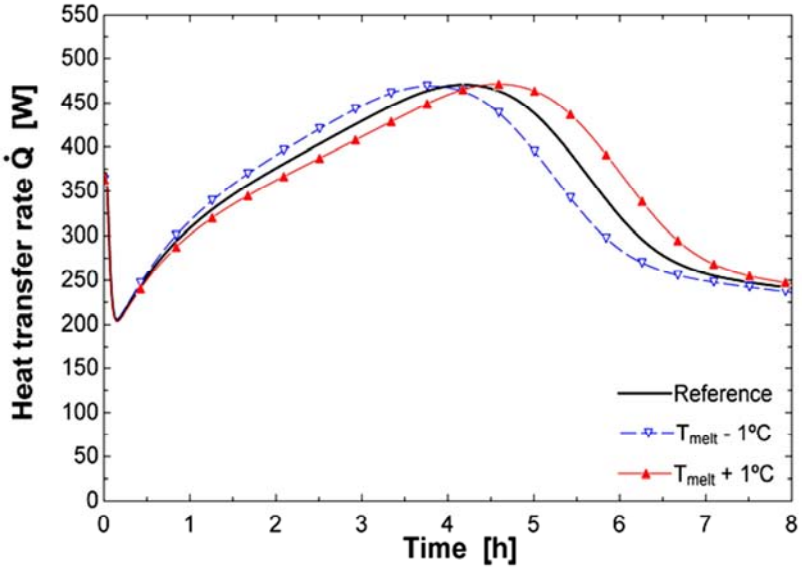

Figure 5

Highlights:

- A model of PCM thermal energy storage for cooling applications is presented
- The error and computational time of the simulations is evaluated
- The effect of the input parameters uncertainty is also analysed
- Some approximations of the parameters give important computational time reduction
- The uncertainty of the inlet HTF temperature presents the highest influence